Structural and comparative study of water confined in a mesoporous bioglass by X-ray total scattering

A. Rjiba, J. Jelassi, N. Letaief, A. Lucas-Girot, Sébastien Pillet, Dominik Schaniel, E-E Bendeif, R. Dorbez-Sridi

Structural and comparative study of water confined in a mesoporous bioglass by X-ray total scattering

A. Rjiba[a], J. Jelassi[a], N. Letaief[a,b], A. Lucas-Girot[b], S. Pillet[c], D. Schaniel[c], E-E. Bendeif[c *] and R. Dorbez-Sridi[a].

[a] Laboratoire Physico-Chimie des Matériaux, Département de Physique, Faculté des Sciences de Monastir, Avenue de l'environnement, 5019 Monastir, Tunisie.

[b] Institut des Sciences Chimiques de Rennes, UMR 6226 CNRS/Université de Rennes 1, Rennes Cedex, France.

[c] Université de Lorraine, CRNS, CRM2, UMR 7036, F-54506 Nancy, France,

Abstract:

The structural properties of water confined in two silica matrices characterised by well-controlled organised porosity with a narrow pore size distribution: i) a new mesoporous bioactive glass (MBG 92S6) and ii) SiO_2 MCM-41 were studied using laboratory total X-ray scattering coupled to molecular pair distribution function (PDF). The PDF analysis shows that the hydrophilic/hydrophobic character of the water-bioglass interface affects the structural properties of the confined water in the same way as water confined in different mesoporous matrices presenting an intermediate hydrophilic and hydrophobic interface regardless of their pore size and distribution. We also compare the effect of the confinement inside MBG 92S6 and different mesoporous hydrophilic and hydrophobic silica matrices. We show that the pore surface properties have a stronger influence on the structural organisation of the confined water than the pore size distribution.

Keywords: Bioactive glasses, sol-gel chemistry, X-ray total scattering, PDF analysis, Solid-state NMR

I. Introduction

Significant advances in the development of Mesoporous Bioactive Glasses (MBGs) based on conventional silica mesoporous materials such as SBA-15 or MCM-41 have been made in the last two decades **[1-7]**. These biomaterials have a huge potential in the field of biomedicine, e.g., for bone tissue regeneration, drug and gene deliveries, DNA vaccination or cellular treatment **[8-15]**. The glass bioactivity is usually evaluated by measuring the rate of HCA (Hydroxy-Carbonate Apatite) formation at the bioactive glass surface on its exposure either to body fluids in vivo or to a simulated body fluid (SBF) in vitro **[16-17].** These nanostructured materials are also characterized by an excellent thermal and mechanical stability. They further present a highly ordered mesoporous arrangement, a unique pore-wall structure and a large amount of internal hydroxyl (silanol), which results in a large surface area and porosity magnitudes higher than those obtained by conventional methods (melt-prepared bioactive glasses). In addition, functionalization, drug delivery properties and hemostatic activity **[18-21]** depend on interactions with guest molecules, which are usually established through electrostatic attractive interactions, hydrophilic–hydrophobic forces or electronic interactions **[22-24]**.

It has been shown that the introduction of new atoms such as Ca, P or Na in the SiO_2 network results in a higher bioactive response (i.e. faster formation of HCA layers) without altering the surrounding fluids **[25-28]**. At the atomic scale, the silica network is modified: P_2O_5 is added initially as network formers and CaO is incorporated into the system as a network modifier **[29]**. In fact, the introduction of alkali and alkaline earth metal oxides ions into the bioglass modifies the silicate network polymerization by breaking Si–O–Si bonds, where bridging oxygen (BO) atoms will convert into non-bridging oxygen (NBO) anions. These modifications lead to five structural units related to the SiO_4 tetrahedron are denoted as $Q_i(Si)$ (*i = 0, 1, 2, 3, 4*), where *i* represents the number of bridging oxygen atoms (BO) per Si atom thereby leading to *4–i* positions occupied by non-bridging oxygen (NBO) ions. On the other hand, the effect of the P_2O_5 content on the structure of glasses with low content of P_2O_5 has been discussed in detail by Garcia *et al* **[30]**. It has been shown that phosphorous is present as a separate amorphous calcium

orthophosphate phase (CaP), which is dispersed over the pore wall as nanometer-sized clusters interrupting the dominating CaO-SiO_2 pore wall builder **[31]**.

When non-ionic triblock copolymers such as P123, are added in the synthesis medium the resulting porous structure depends on the hydrogen-bond interactions with the solvent: in the case of a binary system SiO_2-CaO one obtains a 2-D hexagonal hydrophilic structure, whereas the binary system SiO_2-P_2O_5 leads to the formation of a 3-D cubic hydrophobic mesostructure. Finally, in the case of the ternary system SiO_2-CaO-P_2O_5, the presence of CaO and P_2O_5 leads to the formation of hydrophilic 2D-hexagonal or hydrophobic 3D-cubic, or even mixed mesoporous structures depending on the solvent evaporation temperature **[30-32].** Consequently, the structural properties of water confined in such MBGs are altered compared to conventional silica mesoporous materials. Furthermore, it has been shown that the intermolecular interactions at the water-bioglass interface affect the structural and dynamical properties of confined water **[33-37]**. All these features clearly highlight the importance of the various structural characteristics of biomaterials on the final properties. Since these materials are intended to interact with body fluids which are essentially composed of water, it is then crucial to study and understand the water-MBG interactions. It is especially important to assess whether and to what extent the hydration process may affect the biodegradation and the reactivity of these biomaterials. Thus, the identification and characterization of the active surface sites directly involved in the glass bioactivity mechanism based on their interactions with water molecules is essential for further progress in this field.

So far, only few studies have been carried out to elucidate the structural arrangement of water molecules confined in such MBGs samples and then on critical properties of these biomaterials, such as biodegradation and bioactivity. To investigate structural, dynamical, and physical properties of water confined in silica nanopores of various sizes and geometries, generally molecular simulations have been employed to approximate a realistic interface that present hydrophilic/hydrophobic features. Bonnaud *et al* **[38]** have investigated the structural and dynamical properties of water confined within a model of slit silica nanopores where all the hydrogen atoms of the hydroxylated surface are removed and the negative charge of the resulting oxygen dangling bonds is compensated by Ca^{2+}counterions. They have shown that the water structure and orientational

ordering with respect to the matrix surface is much more disturbed, while water dynamics is slowed down and vicinal water molecules stick to the pore surface over longer times than in the case of hydroxylated silica surfaces. Ladanyi et al **[39]** carried out ns MD simulations of 2, 3, and 4 nm diameter pores of silica with a low density of silanol functional groups. They found that water molecules form two distinct molecular layers at the interface and exhibit a uniform density in the core region, but somewhat lower than in the bulk liquid. Renou *et al* **[40]** have investigated the structural properties of water confined within three different matrixes: a protonated mesoporous material (PP, with SiOH groups), a deprotonated material (DP, with negatively charged surface groups), and a compensated-charge framework (CC, with sodium cations compensating the negative surface charge). They demonstrate that the structure of water inside the different pores shows significant differences in terms of layer organization and hydrogen bonding network.

In view of the results of these simulations concerning the structural behavior of confined water in silica matrices, it is important to study experimentally the structural properties of confined water. We therefore investigate the structural properties of confined water inside two mesoporous glasses having the same structural features but different chemical composition: i) a conventional silica mesoporous material MCM-41 and ii) a ternary Mesoporous Bioactive Glass (SiO_2-CaO-P_2O_5 with a molar ratio of Si/Ca/P = 92/6/2, named hereafter 92S6). Thereby we elucidate the effect of different modifier species present at the surface of the host matrix on the structural properties of confined water. The structural characterization is performed by combining solid-state nuclear magnetic resonance (NMR) spectroscopy and X-ray total scattering experiments coupled to pair distribution function (PDF) analysis.

2.Experimental methods

2.1 Synthesis

2.1.1SiO_2 MCM-41:

The synthesis of SiO_2 MCM-41 was performed according to the protocol of Beck *et al* **[42]**

2.1.2. Mesoporous bioactive glass (92S6)

Mesoporous 92S6 was synthesized according to the procedure previously published **[42-43]** by a two-step acid-catalyzed self-assembly process combined with hydrothermal treatment in an inorganic-organic system. The P123 amphiphilic block copolymer: poly(ethylene oxide)-block-poly(propylene oxide)-block-poly(ethylene oxide) (PEO-PPO-PEO) was used as organic structure-directing agent. The reactants tetraethyl orthosilicate (TEOS, 99%; Aldrich, France), Triethyl phosphate (TEP, 99.8%; Aldrich, France), $Ca(NO_3)_2$,$4H_2O$ (≥ 99%, Fluka, Germany), P123 were used without further purification. (92S6 was prepared by dissolving 6 g of P123 in 120 ml of 2 M HNO_3 and 30 ml of distilled water solution, under stirring at 40°C until the solution became clear. Then 3.6 g of TEOS, 0.16 g of TEP and 0.53 g of $Ca(NO_3)_2$, $4H_2O$ (to obtain a molar ratio of Si/Ca/P = 92/6/2) were added to the prepared aqueous solution. The final pH was 0.3. The mixture was stirred at 40°C for 12h, and then hydrothermalized at 100°C for 48h. Without any filtering and washing, the resulting precipitate was directly dried at 100°C for 20 h in air. The as-synthesized powders were calcined at 650°C in air for 6 h in order to remove completely the organic structure-directing agent.

2.1.3 Mesoporous non-modified and modified silica gels

Mesoporous silica gels are commercially available and consist of an interconnected disordered porous network. Silica gel (35–70 μm, >99.5% SiO_2, Grace Davison SI 1404) with a mean pore diameter in the range of 5–7 nm was used. This hydrophilic matrix was hydrophobized by dropwise addition of 5.25 ml trimethylchlorosilane ($(CH_3)_3SiCl$, TMCS, 99% pure, Aldrich) to 8.67 g of silica in a mixture of 50 ml water (doubly distilled) and 21.6 ml of isopropanol (Aldrich, 99.9% pure) and subsequently refluxed for 30 min during continuous stirring. Prior to the TMCS

addition, the material was left in the liquid mixture for 5 min. After modification, the materials were dried, washed three times with water/ethanol, and dried in air at 393 K. The untreated silica provides the hydrophilic matrix, classed as "non-modified." The treated sample with a predominantly hydrophobic interface provides the "modified" sample material with a methylated surface layer of 3 Å thickness **[44]**.

2.2. Characterization of the mesoporous matrices

In order to determine the textural parameters of the four mesoporous silica samples (MCM-41, 92S6, non-modified and modified silica gels) we performed nitrogen adsorption/desorption isotherms using Brunauer-Emmet-Teller (BET) measurements **[45]** and Barrett-Joyner-Halenda (BJH) analysis **[46]**.

Prior to experiments, the samples were out-gassed at 200 °C for 24h. The specific surface area was obtained by the BET analysis, while the pore size diameter and distribution were calculated from the BJH fits of the desorption isotherms between $P/P_0 = 0.350$ and 0.999 assuming cylindrical pores with both sides open. The results are summarized in **Table I**.

Table I: *Textural parameters of silica gels and glasses: specific pore volume (V_{pore}), median pore diameter (D_{pore}) and Specific surface area (S_{BET}).*

Sample	V_{pore} (cm^3/g)	D_{pore} (nm)	S_{BET} (m^2/g)	Pore distribution
Non modified silica gel	0.84	*6.09*	472	*disordered*
modified silica gel	0.75	*5.96*	438	*disordered*
MCM-41	0.79	*3.8*	825	*2D hexagonal*
92S6	0.66	*5.7*	376	*2D hexagonal*

2.3. Total X-ray scattering measurements:

The total scattering X-ray measurements have been performed on a laboratory X-ray diffractometer (PANalyticalX'Pert PRO) using the Debye-Scherrer transmission set up and Mo Kα radiation (λ = 0.71073 Å). Different optical components can be used on the incident and diffracted beam, e.g. the divergence

slit of 0.02 mm and additional shielding were applied to the optical path in order to achieve a feature-free background. The used experimental setup allows to collect total scattering data up to 2θ angle of 150 degrees corresponding to a maximum scattering vector Q of ~17 $Å^{-1}$. We note here that the total scattering measurements have been conducted under the same experimental conditions for all the studied samples (MCM-41, 92S6 and bulk water). The collected data were then corrected for experimental effects (absorption, multiple scattering, polarization, Compton scattering and Laue diffuse scattering) and the scattering signal from the air and the experimental set up was measured independently under the exact same conditions as the samples and subtracted as a background in the data reduction procedure. For obtaining the experimental atomic pair distribution function G(r) by a direct sine Fourier transformation of the resulting total scattering structure function S(Q), the data were truncated at a finite maximum value of Q_{max}=14 $Å^{-1}$ beyond which the signal-to-noise ratio became unfavourable. All data processing was done using Highscor and PDFgetX2 softwares **[47]**.

The diffraction pattern for the confined water is obtained by subtracting the data for the "dry" sample from that of the "wet" sample using appropriate attenuation factors. This procedure eliminates the silica–silica correlations, but takes no account of possible cross-terms for water–silica correlations.

Prior to the hydration process, the samples were dried at 200 °C for three days in an oven to remove the residual adsorbed water molecules.

The measurements were performed for the dry and the wet samples, hydrated with H_2O to give a filling factor of 0.5. The filling factor **f** is defined by $\mathbf{f = V/V_p}$ where **V** is the volume of added water and $\mathbf{V_p}$ is the pore volume corresponding to the used sample. The choice of **f = 0.5** was made to coincide with one of the filling factors used in the earlier studies and to emphasize the features for a water layer thickness [8–9 Å] that has relevance to many biological applications.

3. Results and discussion

Figure 1 shows the pair correlation function of the confined water derived from the corresponding structure factor. The pair correlation function of bulk water is shown in the same figure for comparison. One notes that the bulk water has a tetrahedral local structure that exhibits the following features: the first molecular neighbors are

located at a distance (O—O distance) of 2.82 Å from each other and the second neighbors are approximately at 4.5 Å (**Figure 1**). These results are in perfect agreement with those reported in the literature **[48-49].**

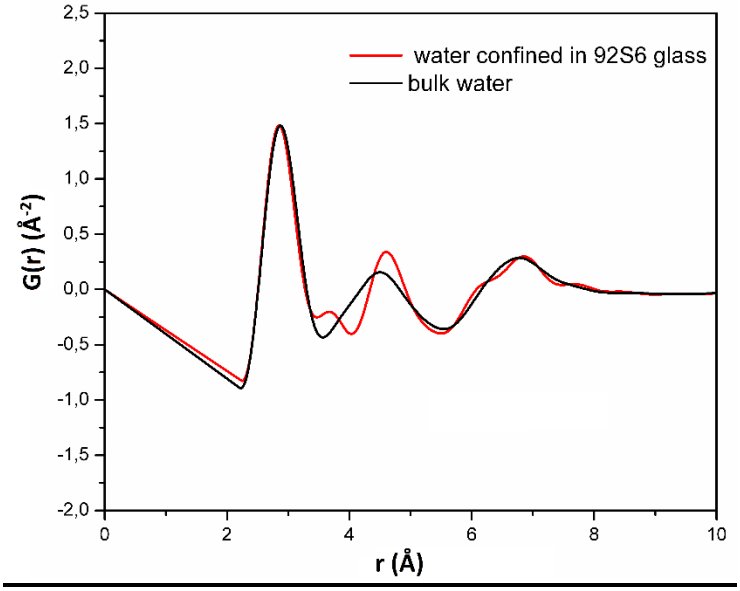

Figure 1*. The pair correlation function G(r), obtained from total X-ray scattering at 297 K of: Water confined in 92S6 bioglass hydrated at 50% (red line), bulk water (black line)*

The confinement effect of water in the 92S6 glass is clearly visible in the r range of 3-6 Å (**Figure 1**). The tetrahedral arrangement of confined water shows an additional peak at 3.65 Å compared to the bulk water. One further notes that the first neighboring water molecules (at 2.82 Å) are not affected by the confinement, however the second neighboring water molecules are located on two different sites at 3.65 Å and 4.6 Å respectively. This new distribution is the signature of the structural rearrangement of the hydrogen-bonding network induced by the water-MBG surface interactions and/or confinement effect.

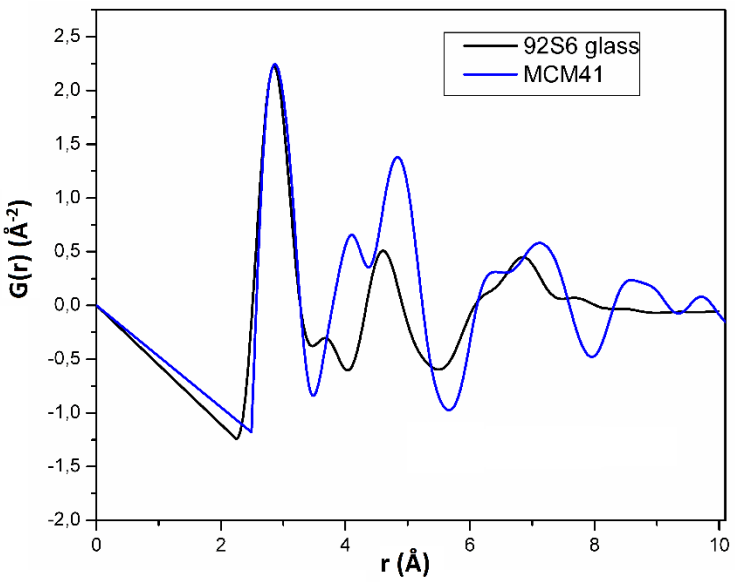

Figure 2. *The pair correlation function G(r), obtained from total X-ray scattering data at 297 K for water confined in: 50% hydrated 92S6 bioglass (black line) and in the 50% hydrated MCM-41 glass (blue line)*

To better understand the new structure of water molecules within the glass 92S6 nanopores, we compared these results with those obtained on MCM-41 (**Figure 2**). It is well known that the local order of confined water depends on the hydrophilic or hydrophobic character of the host matrix. Despite the similar high surface area , the high porosity and the well-ordered distribution of mesopores in both 92S6 and MCM-41 glasses, the water confined in the 92S6 glass shows different structural features (in the 3-6 Å range) compared to that confined in MCM-41 which are in agreement with those obtained by Yamaguchi and coworkers **[50**]. The water structural changes, caused by the vicinity of the confinement surface, are especially reflected by a rearrangement of the second water neighbours. Compared to the results in MCM-41 the second neighbors located at 4 Å and 4.8 Å, are shifted to 3.7 Å and 4.6 Å in the case of 92S6 MBG (**Figure 2**). These shifts can be explained by the host-guest surface interactions. In fact, due to the presence of CaP clusters at the wall interface, 92S6 glass prepared at intermediate evaporation temperature, presents a hydrophilic/hydrophobic character in contrast to the purely hydrophilic sample MCM-41. The surface effects influence not only the translational, but also the rotational degrees of freedom of water molecules. In this context, it has been shown from MD studies performed by Brovchenko *et al* **[51]** and Gallo *et al* **[52]** that the distribution of the O–O–O angle between three neighboring water

molecules in the center of the pore is similar to bulk water, with a maximum correspondence of the angle characteristic of tetrahedral coordination. The distribution of the O–O–O angle becomes flat for water molecules approaching the pore wall confirming that the relative orientations of neighboring water molecules are strongly affected by the presence of the hydrophilic silica surface in the case of the MCM-41 matrix for which the tetrahedral coordination breaks down. The authors interpreted this effect by the two-dimensional character of the adsorbed thin film of water.

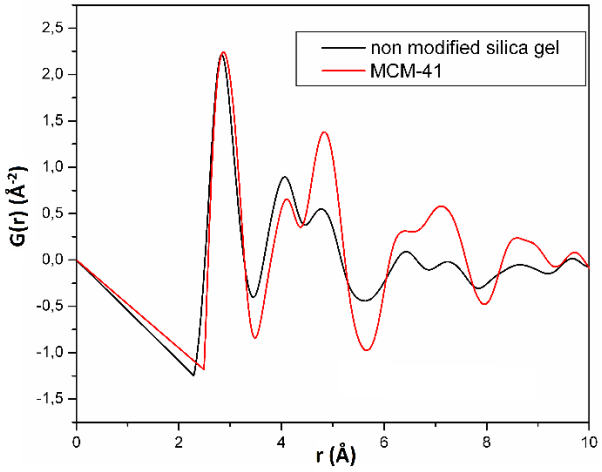

***Figure 3**: The pair correlation function G(r), obtained from total X-ray scattering data at 297K for water confined in: 50% hydrated MCM-41 (red line), 50% hydrated non modified silica gel obtained by Jelassi et al **[55]** (black line)*

This same structure was observed for water confined in a hydrophilic mesoporous silica gel (non-modified silica gel) (**Figure V) [55]** with an average pore diameter of 6 nm.

In spite of a different pore distribution: well ordered in the MCM-41 and random in the non-modified silica gel, water is structured in the same way in both matrices. This might be explained by the fact that the hydroxyl groups present at the charged surface of the pores can act as donors or acceptors of hydrogen bonds involving confined water molecules.

In order to study the influence of the hydrophilic/hydrophobic nature of the pores on the structuration of confined water molecules, we compare the results of this study to those obtained for the modified silica gel matrices with different pore organization and distribution **[44]**. One notes that the modified silica gel matrix is characterized by randomly distributed pores with similar mean pore diameters of

~6 nm. In contrast, the studied 92S6 MBG presents a well-ordered hexagonal network, with a mean pore diameter in the range of 5-7 nm. Figure VI shows the comparison of the mesoporous matrices: the modified (hydrophobic) and 92S6 MBG.

We observe that the rearrangement of the confined water in the modified silica gel matrix exhibits similar features as for 92S6 MBG. Indeed, the PDF peaks corresponding to the second water neighbors are located at 3.65 Å and 4.61 Å for the 92S6. These pics are shifted to 3.55 Å and 4.5 Å for the modified hydrophobic matrix.

In contrast to the hydrophilic matrix, when water molecules are in contact with hydrophobic walls (modified silica gel) (**Figure 4)**, the interaction forces, which are primarily of Van der Waals type, are less important and the water molecules at the water-bioglass interface are differently oriented to create a hydrogen-bond network linked more directly to the rest of the water volume. At the molecular level, the interactions between confined water and a hydrophobic surface are characterized by a decrease in the entropy due to the reorganization of the water molecules in a specific configuration to compensate the loss of hydrogen bonds with the polar groups of the hydrophobic surface. This effect is manifested by the reappearance of the peak at 3.65 Å in the PDF of water confined in MBG 92S6, and is similar to what occurs when pressure is applied to bulk water and indicates a substantial distortion of the hydrogen bond network **[53-54]**.

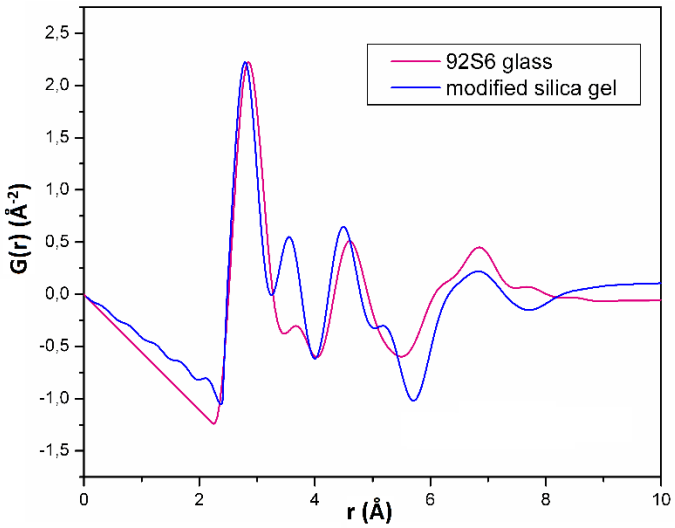

***Figure 4**. The pair correlation function G(r), obtained from total X-ray scattering data at 297K for water confined in: 50% hydrated 92S6glass (pink line), 50% hydrated modified silica gel obtained by Jelassi et al **[55]** (blue line)*

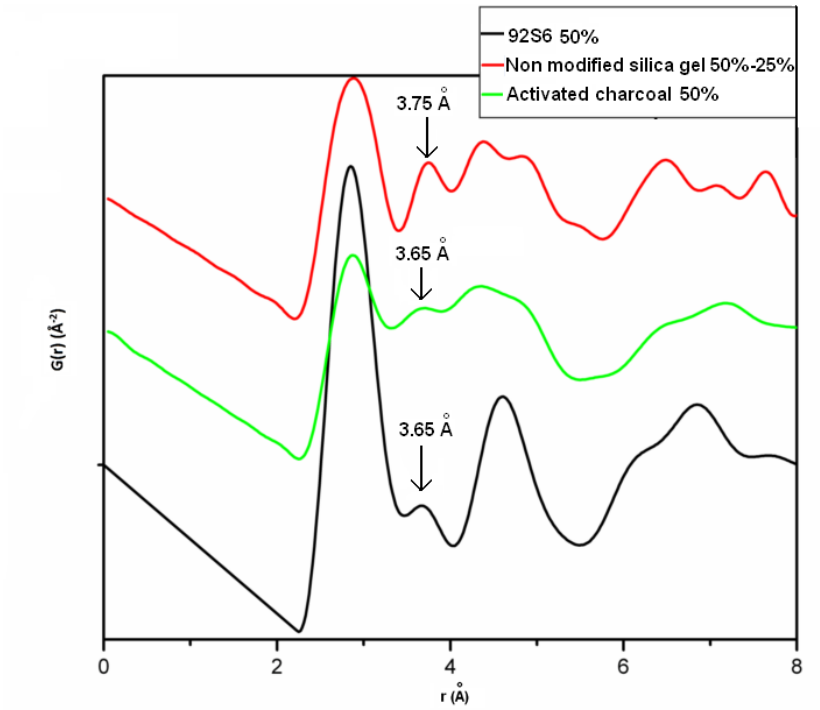

***Figure 5**. The pair correlation function G(r), obtained from total X-ray scattering data at 297K for water confined in: 50% hydrated 92S6 glass (black line),50% hydrated activated charcoal[59] and subtraction of non-modified silica gel hydrated at 50%-25%*

This result indicates that the pore surface of the 92S6 MBG has a hydrophobic character due to the presence of the CaP groups.

The peak at 3.7 Å could also originate from cross terms between the water molecules and the matrix pore walls. To overcome this ambiguity, a subtraction between the intensities of the non-modified silica gel hydrated to 50% and to 25% was applied [**33**]. This approach aims to minimize the effect of the cross terms. However, two water populations are present inside the pores: water molecules in contact with the silica walls affected by hydroxyl-like interactions with the matrix and a second population at the center of the pores. This subtraction essentially allows a better analysis of the structuration of water molecules in the center of the pores.

Figure 5 shows that the PDF of water confined in 92S6 present some similar features to that of water confined in the activated charcoal wich is purely

hydrophobic and that obtained after subtraction of two signals relative to two hydrations rates of non-modified silica gel (50% and 25%). The differential PDF of the water confined within the non-modified silica pores shows three characteristic peaks: the first one is located at 3.75 Å and the two other peaks are respectively observed at 4.37 Å and 4.85 Å. This result clearly indicates that the first peak in the PDF of water confined in 92S6 MBG corresponds to the water-water interactions and not to Si-O…O cross terms. This distance has already been identified by Gorbaty and coworkers **[53]** in water under high hydrostatic pressure and their results have been interpreted by assuming that the structure of water under pressure is a combination of ice like and a Lennard-Jones-like structures. The authors have ascribed the peak position at 3.65 Å to the O–O distance of "contracted water molecules."

Moreover, one notes that the PDF peaks of 92S6 MBG are located in an intermediate region compared to those of the hydrophilic and the hydrophobic silica matrices. Thus, we can deduce that the pore surface of the bioglass 92S6 has a hybrid character between that of the purely hydrophilic or totally hydrophobic mesoporous silica gel due to the presence of CaP clusters.

In this context, it has been suggested that water molecules next to a hydrophilic surface will tend to orient themselves with one H-bond "vector" pointing toward the wall and the other three toward neighboring water molecules. However, when water molecules are confined in a hydrophobic matrix, the modification of its structure may be attributed to nonbonding water–water distances of water molecules of the affected layer in the outer shell of clusters and where some molecules are constrained to be in interstitial cavities of a tetrahedral configuration. Similar features in the O–O partial pair correlation function of water at high pressure have been obtained by Soper and Ricci from neutron diffraction using H/D substitution **[55]**.

From these results, one can deduce that the character of the pore surfaces has a stronger influence on the structural organization of the confined water than the pore distribution.

4. Conclusion

In summary, we investigated the structural properties of water confined in a new mesoporous bioactive glass 92S6 and in MCM-41 by total X-ray scattering coupled

to PDF analysis. We found that the pore surface of the bioglass 92S6 has a hybrid character between that of the hydrophilic or hydrophobic mesoporous silica gel due to the presence of CaP clusters. We have also shown from the PDF analysis that although the MCM-41 matrix and the bioglass92S6, having the same structural morphology with a well-ordered hexagonal network, the structural properties of the confined water molecules in the two matrices are different. This effect is related to the difference between the pore surface character of both matrices. Furthermore, we compared the structural features of water confined in 92S6 bioglass to those obtained for similar mesoporous hydrophilic and hydrophobic silica matrices with different pore organisation and distribution. A subtraction between the intensities of the non-modified silica hydrated at two levels of hydration was applied. This approach demonstrates that the peak at 3.7 Å present in the PDF of confined water in the 92S6 is not due to the cross-term between the water molecules and the matrix but it is related to the structural reorganisation of water molecules induced by the confinement effect in the mesoporous MBG. Once the water is confined in the mesoporous structure, two effects are present: the effect of confinement and that of surface interaction. We showed that the effect of confinement is more pronounced in hydrophobic/hydrophilic mesoporous matrices than in purely hydrophilic matrices. However, in a hydrophilic mesoporous matrix, the structural organisation of confined water is more affected by the surface effect, nevertheless the effect of confinement is present and it's revealed by a subtraction of the pair correlation function measured for two samples with different hydration levels.

Acknowledgements

We thank Pierrick Durand and the X-ray diffraction platform of the Lorraine University for the total X-ray scattering measurements. This work was supported by the CNRS-DGRST collaborative project N° 15R/1302.

References

[1] O.C. Farokhzad, R. Langer. Adv. Drug Deliv. Rev. 58, 1456, (2006).
[2] J. Andersson, J. Rosenholm, S. Areva, M. Linden. Chem. Mater. 16, 4160, (2004).
[3] C. Barbe, J. Bartlett, L. Kong, K. Finnie, H.Q. Lin, M. Larkin, S. Calleja, A. Bush, G. Calleja. J. Adv. Mater. 16, 1959, (2004).
[4] D. J. Bharali, I. Klejbor, E. K. Stachowiak, P. Dutta, I. Roy, N. Kaur, E. J. Bergey, P. N. Prasad, M. K.Stachowiak, Proc. Natl. Acad. Sci. U.S.A.102, 11539, (2005).
[5] A. L. Doadrio, E. M. Sousa, J. C. Doadrio, J. P. Pérez, I. I. Barba, M.V. Regi, J. Control. Release. 97, 125, (2004).
[6] Y. J. Hwang, O. Chul, S.G. Oh, J. Control. Release.106, 339, (2005).
[7] M. Manzano and M. Vallet-Regi. J. Mater. Chem. 20, 5593, (2010).
[8] F. Rehman, P.L.O. Volpe and C. Airoldi. Colloids and Surfaces B: Biointerfaces. 119, 82, (2014).
[9] I. Slowing, B.G. Trewyn, V.S.Y. Lin. J. Am. Chem. Soc. 128, 14792, (2006).
[10] P. Yang, S. Gai, J. Lin. Chem, Soc. Rev. 41, 3679, (2012).
[11] Z. Li, J.C. Barnes, A. Bosoy, J.F. Stoddart, J.I. Zink, Chem. Soc. Rev. 41, 2590, (2012).
[12] S. Dashi, P.N. Murthy, L. Nath, P. Chowdhury. ActaPolonia Pharm. Drug Res. 67, 217, (2010).
[13] G. Liu, C. Zhu, J. Xu, Y. Xin, T. Yang, J. Li, L. Shia, Z. Guo, W. Liu. Colloids Surf. B111, 7, (2013).
[14] W.B. Liechty, D.R. Kryscio, B.V. Slaughter, N.A. Peppas. Annu. Rev. Chem. Biomol. Eng. 1, 149, (2010).
[15] C. Wu, J. Chang, Y. Xiao. Ther. Deliv. 9, 1189, (2011).
[16] Y. Ebisawa, T. Kokubo,K. Ohura, T. Yamamuro. J. Mater. Sci.Mat. Med, 1, 239, (1990)
[17] S. Fujibayashi, M. Neo, H.-M. Kim, T. Kokubo, T. Nakamura. Biomaterials, 24, 1349, (2003).
[18] J. Sun, Y. S, Li, L..; Li, W. Zhao, L. Li, J. H. Gao, M. L. Ruan,. J. L. Shi. J. Non-Cryst. Solids, 354, 3799, (2008).
[19] L. Z. Zhao, X. X. Yan, X. F. Zhou, L. Zhou, H. N. Wang, J. W. Tang, C. Z. Yu, Microporous and Mesoporous Materials, 109, 210, (2008).
[20] W. Xia, J. Chang. J. Controlled Release, 110, 522, (2006).
[21] T. A. Ostomel, Q. Shi, C. K. Tsung, H. Liang, G. D. Stucky. Small, 2, 1261, (2006).
[22] Vallet-Regí, M. Chem. Eur. J. 12, 5934, (2006).
[23] S. W. Song, K. Hidajat, K and K. Kawi. Langmuir 21, 9568, (2005).
[24] A. Nieto, M. Colilla, F. Balas and M. Vallet-Regí. Langmuir 26, 5038–5049 (2010).
[25] I. Izquierdo-Barba, A. J. Salinas, M. Vallet-Regı´. J. Biomed. Mater. Res. 47, 243, (1999).
[26] A. Martınez, I. Izquierdo-Barba, M. Vallet-Regı´. Chem. Mater. 12, 3080 (2000).
[27] A. J Salinas.;A. I. Martin; M. Vallet-Regı´. J. Biomed. Mater. Res. 61, 524 (2002).
[28] I. Izquierdo-Barba, D. Arcos,Y. Sakamoto,O. Terasaki,A. Lopez-Noriega, M. Vallet-Regı´. Chem. Mater. 20, 3191(2008).
[29] M. Vallet-Regı´, A. J. Salinas and D. Arcos. J. Mater. Sci :Mater. Med. 17, 1011 (2006).
[30] A. Garcı´a, M. Cicuendez, I. Izquierdo-Barba, D. Arcos and M. Vallet-Regı´. Chem. Mater. 2009, 21, 5474–5484

[31] E. Leonova, I. Izquierdo-Barba, D.Arcos, A. Lopez-Noriega, N. Hedin, M.Vallet-Regf, M.Eden. J. Phys. Chem. C . 112, 5552. (2008).
[32] Z. Li, D. H. Chen, B. Tu, D. Y. Zhao. Microporous Mesoporous Mater. 105, 34, (2007).
[33] A. Fouzri, R. Dorbez-Sridi, M. Oumezzine. The European Physical Journal Applied Physics. 22, 21, (2003).
[34] A. Fouzri, R. Dorbez-Sridi, M. Oumezzine. The Journal of Chemical Physics. 116, 791, (2002).
[35] I. C. Bourg, C. I. Steefel. J. Phys. Chem. C. 116, 11556, (2012).
[36] L. Bocquet, E. Charlaix. Chem. Soc. Rev. 39, 1073, (2010).
[37] H. Mosaddeghi, S.Alavi,M.H.Kowsari,B.Najafi. J. Chem. Phys. 137, 647, (2012).
[38] P. A. Bonnaud, B. Coasne, R. J.-M. Pellenq. J. Chem. Phys. 137, 064706, (2012).
[39] A. A. Milischuk., B. M. Ladanyi. J.Chem.Phys. 135, 174709, (2011).
[40] R. Renou, A. Szymczyk, A. Ghouffi. The journal of chemical physics. 140, 044704, (2014).
[41] J. S. Beck, J. C. VartUli, W. J. Roth, M. E. Leonowicz, C. T. Kresge, K. D. Schmitt, C. T-W. Chu, D. H. Olson, E. W. Sheppard, S. B. McCullen, J. B. Higgins, and J. L. Schlenker. J. Am. Chem. SOC., Vol. 114, No. 27, 10835, (1992).
[42] N. Letaïef, A. Lucas-Girot, H. Oudadesse, R. Dorbez-Sridi, P. Boullay. Microporous and Mesoporous Materials. 195, 102, (2014).
[43] N. Letaïef, A. Lucas-Girot, H. Oudadesse, R. Dorbez-Sridi. Materials Research Bulletin. 60, 882, (2014).
[44] Jelassi J, Grosz T, Bako I, et al. Structural studies of water in hydrophilic and hydrophobic mesoporous silicas: an X-ray and neutron diffraction study at 297 K. J Chem Phys. 2011;134(6):064509.
[45] S. Brunauer, P. H. Emmett and E. Teller. J. Am. Chem. Soc. 60, 309, (1938).
[46] E. P. Barret, L. G. Joyner and P. P. Halenda. J. Am. Chem. Soc., 73, 373, (1951).
[47] X. Qiu, J. W. Thompson, S. J. L. Billinge. J. Appl. Cryst. 37, 678, (2004).
[48] A. H. Narten, H. A. Levy. J. Chem. Phys. 55, 2263, (1971).
[49] H. Bertagnolli, P. Chieux, M. D. Zeidler. Mol. Phys. 22, 759, (1976).
[50] P. Smirnov. T. Yamaguchi, S. Kittaka, S. Takahara and Y. Kuroda. J. Phys. Chem. B. 104, N 23, 5498, (2000).
[51] Rieth M, Schommers W. Handbook of theoretical and computational nanotechnology: basic concepts, nanomachines and medical nanodevices. Valencia (CA): American Scientific Publishers; 2005.
[52] P. Gallo, M. A. Ricci and M. Rovere, J. Chem. Phys. 116, 342, (2002).
[53] V. Okhulkov, Y. N. Demianets, and Y. Gorbaty. J. Chem. Phys. 100, 1578, (1994).
[54] R. Dorbez-Sridi, R. Cortes, E. Mayer and S. Pin. J. Chem. Phys. 116, 7269, (2002).
[55] A. Soper and M. A. Ricci, Phys. Rev. Lett. 84, 2881, (1999).